J Neurooncol (2006) 80:111–121
DOI 10.1007/s11060-006-9171-8

LABORATORY INVESTIGATION

Combined low dose ionizing radiation and green tea-derived epigallocatechin-3-gallate treatment induces human brain endothelial cells death

Nancy McLaughlin · Borhane Annabi · Marie-Paule Lachambre · Kwang Sik Kim · Jean-Paul Bahary · Robert Moumdjian · Richard Béliveau

Received: 27 February 2006 / Accepted: 30 March 2006 / Published online: 19 May 2006

Abstract The microvasculature of brain tumors has been proposed as the primary target for ionizing radiation (IR)-induced apoptosis. However, the contribution of low dose IR-induced non-apoptotic cell death pathways has not been investigated. This study aimed to characterize the effect of IR on human brain microvascular endothelial cells (HBMEC) and to assess the combined effect of epigallocatechin-3-gallate (EGCg), a green tea-derived anti-angiogenic molecule. HBMEC were treated with EGCg, irradiated with a sublethal (≤10 Gy) single dose. Cell survival was assessed 48 h later by nuclear cell counting and Trypan blue exclusion methods. Cell cycle distribution and DNA fragmentation were evaluated by flow cytometry (FC), cell death was assessed by fluorimetric caspase-3 activity, FC and immunoblotting for pro-apoptotic proteins. While low IR doses alone reduced cell survival by 30%, IR treatment was found more effective in EGCg pretreated-cells reaching 70% cell death. Analysis of cell cycle revealed that IR-induced cell accumulation in G2-phase. Expression of cyclin-dependent kinase inhibitors p21(CIP/Waf1) and p27(Kip) were increased by EGCg and IR. Although random DNA fragmentation increased by approximately 40% following combined EGCg/IR treatments, the synergistic reduction of cell survival was not related to increased pro-apoptotic caspase-3, caspase-9 and cytochrome C proteins. Cell necrosis increased 5-fold following combined EGCg/IR treatments while no changes in early or late apoptosis were observed. Our results suggest that the synergistic effects of combined EGCg/IR treatments may be related to necrosis, a non-apoptotic cell death pathway. Strategies sensitizing brain tumor-derived EC to IR may enhance the efficacy of radiotherapy and EGCg may represent such a potential agent.

Keywords Human brain endothelial cells · Radiotherapy · Green tea · Necrosis · Cell death

Abbreviations

EC	endothelial cells
EGCg	epigallocatechin-3-gallate
GBM	glioblastoma multiforme
HBMEC	human brain microvascular endothelial cells
HUVEC	human umbilical vein endothelial cells

N. McLaughlin · M.-P. Lachambre · R. Béliveau (✉)
Laboratoire de Médecine Moléculaire, Centre de Cancérologie Charles-Bruneau, Hôpital Sainte-Justine-UQAM, Succ. centre-ville, C.P. 8888, H3C 3P8 Montréal, Québec, Canada
e-mail: oncomol@er.uqam.ca

R. Moumdjian · N. McLaughlin
Surgery Department, Neurosurgery Service, Centre Hospitalier de l'Université de Montréal, Montreal, Quebec, Canada

B. Annabi
Laboratoire d'Oncologie Moléculaire, Département de Chimie, Centre BioMed, Université du Québec à Montréal, Montreal, Quebec, Canada

K. S. Kim
Division of Pediatrics Infectious Diseases, The John Hopkins University School of Medicine, Baltimore, MD, USA

J.-P. Bahary
Radio-oncology Department, Centre Hospitalier de l'Université de Montréal, Montreal, Quebec, Canada

IR ionizing radiation
VEGF vascular endothelial growth factor

Introduction

Malignant gliomas, especially glioblastomas multiforme (GBM), are among the tumors most resistant to radiotherapy and chemotherapy [1]. Even in the group with the best prognosis, the median survival rarely exceeds 1 year [2, 3]. Malignant gliomas are also amongst the most intensively vascularized solid tumors [4]. The process of angiogenesis is essential for tumor progression from microscopic cell clusters, receiving nutrients and oxygen by passive diffusion, to macroscopic foci supplied by blood vessels [5]. Furthermore, malignant gliomas become more angiogenic with increasing tumor grade, suggesting that the vascular component plays an important role in their malignant progression [6]. Indeed, GBMs' cell proliferation, invasiveness and necrosis, three facets of gliomas' malignant phenotype, are directly related to brain tumor microvasculature [7].

Radiotherapy is a widely used adjuvant therapy for malignant brain tumors [1] and is believed to exert its anti-cancerous effects by targeting tumor cells [8, 9]. However, recently, it has been proposed that IR might prevent tumor growth or cause tumor regression by targeting tumor vasculature [10]. Indeed, studies have shown that radiotherapy can selectively target endothelial cells (EC) and associated angiogenesis of residual tumor [7]. Tumor-associated EC have a proliferation rate up to 20 times greater than the proliferation rate of normal vasculature [11], rendering them more radiosensitive than non-dividing cells [12]. In addition, EC are generally well oxygenated, which makes them more radiosensitive than poorly oxygenated tumor cells because the oxygen present at the time of radiation may contribute to the formation of cytotoxic molecules and prevent the reversal of some chemical changes [12, 13]. Many investigators have found that IR exposure induces apoptosis in EC [14–17], and that this event precedes tumor cell apoptosis [18]. The occurrence of EC death following IR is a critical factor for both tumor survival following IR and for tumor growth. While toxic insults or physical damage have been found to initiate cellular necrosis [19], the impact of IR-induced cellular damage resulting in non-apoptotic pathways such as necrosis has not been yet investigated in EC.

Targeting tumor-associated EC as part of cancer treatments is an appealing prospect. Antiangiogenic agents have been used successfully in combination with IR to increase the therapeutic efficacy of radiation exposure [20, 21]. Only recently have the EC been considered not only the target of antiangiogenic agents but also of IR and therefore a powerful new potential treatment target in highly vascularized tumors such as glioblastomas [4]. Recent reports have proposed that some naturally occurring phytochemicals can function as sensitizers, augmenting the effectiveness of conventional radiotherary [22–24]. Epigallocatechin-3-gallate (EGCg), a green tea-derived molecule, has been recognized as having many biochemical functions including inhibition of tumor cell growth [8, 24], cell cycle arrest [25–27], induction of apoptosis [24, 28, 29], inhibition of invasion and metastasis [30, 31] and inhibition of angiogenesis [29, 32]. Moreover, we have shown that EGCg suppressed vascular endothelial growth factor (VEGF) receptor function in EC [33] and that EGCg efficiently targeted human EC that escaped IR-induced damage [34]. Whether this natural polyphenol can be used to potentiate IR effects on human brain EC is unknown. Although the human brain microvascular endothelial cells (HBMEC) model, used in this study, is a surrogate model that only approximates tumor-derived EC, it is to our knowledge, the closest in vitro model that can approximate the human brain tumor-derived EC phenotype in long term studies. The goal of this study is thus to characterize the impact of irradiation on HBMEC and to determine whether EGCg can optimize this effect.

Materials and methods

Materials

(−)-Epigallocatechin 3-gallate (EGCg), sodium dodecylsulfate (SDS) and bovine serum albumin (BSA) were purchased from Sigma (Oakville, ON). Mouse anti-p21 monoclonal antibody, rabbit anti-p27 polyclonal antibody and rabbit anti-Caspase-9 polyclonal antibody were from Cell Signaling Technology (Beverly, MA), rabbit anti-Caspase-3 polyclonal and mouse anti-cytochrome C monoclonal antibody were from BD Pharmingen (Mississauga, ON) and mouse anti-GAPDH monoclonal antibody was from Advanced Immunochemical Inc. (Long Beach, CA). Horseradish peroxidase-conjugated donkey anti-rabbit or anti-mouse IgG were obtained from Jackson Immunoresearch Laboratories (West Grove, PA). BCA protein assay kit was purchased from Pierce (Rockford, IL) and enhanced chemiluminescence (ECL)-Western blot kit from Chemicon International

(Temecula, CA). Products for electrophoresis were bought from Bio-Rad (Mississauga, ON) and polyvinylidene difluoride (PVDF) membranes were from Boehringer Mannheim. Trypsin was from Invitrogen (Burlington, ON).

Cell culture

Human brain microvascular endothelial cells (HBMEC) were generated and characterized by Dr Kwang Sik Kim from the John Hopkins University School of Medicine (Baltimore, MD). These cells were positive for factor VIII-Rag, carbonic anhydrase IV, Ulex Europeus Agglutinin I, took up fluorescently labeled acetylated low-density lipoprotein and expressed gamma glutamyl transpeptidase, demonstrating their brain EC-specific phenotype [35]. HBMEC were immortalized by transfection with simian virus 40 large T antigen and maintained their morphologic and functional characteristics for at least 30 passages [36]. HBMEC were maintained in RPMI 1640 (Gibco, Burlington, ON) supplemented with 10% (v/v) fetal bovine serum (FBS) (HyClone Laboratories, Logan, UT), 10% (v/v) NuSerum (BD Bioscience, Mountain View, CA), modified Eagle's medium nonessential amino acids (1%) and vitamins (1%) (Gibco), heparin (5 U/ml) (Gibco), sodium pyruvate (1 mM), L-glutamine (2 mM) (Gibco), EC growth supplement (30 μg/ml), 100 units/ml penicillin and 100 μg/ml streptomycin. Culture flasks were coated with 0.2% type-I collagen to support the growth of HBMEC monolayers. Cells were cultured at 37°C under a humidified atmosphere containing 5% CO_2. All experiments were performed using passages 15 to 28.

EGCg and irradiation treatment

Cells were treated in serum-free RPMI supplemented (or not) with 3–30 μM EGCg for 6 h and were overlaid with medium. Cells were irradiated with a 6 MV photon beam from an Elekta SL75 linear accelerator. The delivered radiation doses were measured using a thermoluminescence dosimetry (TLD) system with an accuracy of 7%. After irradiation, serum-free medium was replaced by RPMI containing 10% FBS and 10% NuSerum and cultures were left to recuperate for 48 h. Non-irradiated control cells were handled similarly to the cells which were subjected to EGCg and/or IR treatments.

Cell survival assay

The extent of cell survival was assessed at either 1 or 48 h after irradiation. Cells were collected by gentle scraping and were resuspended in the overlaying medium. From each experimental sample, 150 μl homogenate were reserved for nuclear cell counting using an automatic cell counter (New Brunswick Scientific Co., Edison, NJ). Viable cell number determination was also assessed using Trypan blue dye solution for exclusion of dead cells.

Analysis of cell cycle by flow cytometry

Distribution of HBMEC throughout the cell cycle was assessed by flow cytometry 48 h after EGCg and/or IR treatments. No serum-fasting preparation was performed prior to analysis and therefore the cell populations were asynchronous. Cells were harvested by gentle scraping, pelleted by centrifugation, washed with ice-cold PBS + EDTA (5 mM), then resuspended in 1 volume PBS/EDTA and fixed with 100% ethanol overnight. Three volumes of staining solution, containing propidium iodide (50 μg/ml) (Sigma) and DNAse-free RNAse (20 μg/ml), were added. The fraction of the population in each phase of the cell cycle was determined as a function of the DNA content using a Becton Dickinson FACS Calibur flow cytometer equipped with CellQuest Pro software. In particular, the characteristics of cell distribution in the sub-G1 region were studied on the DNA histogram.

Fluorimetric caspase-3 activity assay

HBMEC were grown to 60% confluence and treated with EGGg and/or exposed to IR. Cells were collected and washed in ice-cold PBS pH 7.0. Cells were subsequently lysed in Apo-Alert lysis buffer (Clontech, Palo Alto, CA) for 1 h at 4°C and the lysates were clarified by centrifugation at 16,000 g for 20 min. Caspase-3 activity was determined by incubation with 50 μM of the caspase-3-specific fluorogenic peptide substrate acetyl-Asp-Glu-Val-Asp-7-amino-4-trifluoromethylco umarin (Ac-DEVD-AFC) in assay buffer (50 mM Hepes–NaOH (pH 7.4), 100 mM NaCl, 10% sucrose, 0,1% 3-[(3-cholamidopropyl) dimethylammonio]-1-propanesulfonate, 5 mM DTT and 1 mM EDTA) in 96-well plates. The release of AFC was monitored for at least 30 min at 37°C on a fluorescence plate reader (Molecular Dynamics) (λ_{ex} = 400 nm, λ_{em} = 505 nm).

Immunoblotting procedures

Cell lysates were separated by SDS-polyacrylamide gel electrophoresis (PAGE). After electrophoresis, proteins were electrotransferred onto polyvinylidene difluoride membranes which were then blocked overnight

at 4°C with 5% non-fat dry milk in Tris-buffered saline (150 mM Tris, 20 mM Tris–HCl, pH 7.5) containing 0.3% Tween-20 (TBST). Membranes were then washed in TBST and incubated with the primary antibodies (1/1000 dilution) in TBST containing 3% bovine serum albumin, followed by a 1 h incubation with horseradish peroxidase-conjugated anti-rabbit or anti-mouse IgG (1/2500 dilution) in TBST containing 5% non-fat dry milk. The secondary antibodies were visualized by ECL and quantified by densitometry.

Analysis of apoptosis by flow cytometry

Cell death was assessed 48 h after irradiation by flow cytometry. Cells floating in the supernatant and adherent cells harvested by trypsin solution were gathered to produce a single cell suspension. The cells were pelleted by centrifugation and washed with PBS. Then, 2×10^5 cells were pelleted and suspended in 200 µl of buffer solution and stained with annexin V-fluorescein isothiocyanate (FITC) and propidium iodide (PI) as described by the manufacturer (BD Bioscience). The cells were diluted by adding 300 µl of buffer solution and processed for data acquisition and analysis on a Becton Dickinson FACS Calibur flow cytometer using CellQuest Pro software. The *X*- and *Y*-axes indicated the fluorescence of annexin-V and PI respectively. It was possible to detect and quantitatively compare the percentages of gated populations in all of the four regions delineated. In the early stages of apoptosis, phosphatidylserine is translocated to the outer surface of the plasma membrane, which still remains physically intact. As annexin-V binds to phosphatidylserine but not to PI, and the die is incapable of passing the plasma membrane, it is excluded in early apoptosis (annexin-V^+/PI^-). Cells in late apoptosis are stained with annexin-V and PI (annexin-V^+/PI^+). Necrotic cells have lost the integrity of their plasma membrane and are predominantly stained with PI (annexin-V^-/PI^+).

Statistical data analysis

Data are representative of three or more independent experiments. Statistical significance was assessed using Student's unpaired *t*-test and was used to compare the relative proliferation rates. Probability values of less than 0.05 were considered significant. In each figure the statistically significant differences are identified by an asterisk (*) for EGCg or IR treatment compared to control, while a double asterisk (**) shows significance between combined EGCg/IR treatment and either EGCg or IR treatment alone.

Results

Combined EGCg treatment and ionizing radiation exposure reduce HBMEC survival

We examined HBMEC survival in response to either EGCg treatment or IR exposure. Cell survival was assessed immediately after EGCg treatment or 48 h after recuperation in medium with serum. Immediately after EGCg treatment, there was a dose-dependent decrease in cell survival with increasing EGCg concentrations, reaching a maximum effect of 30% decrease at 30 µM EGCg (Fig. 1A, left panel, white

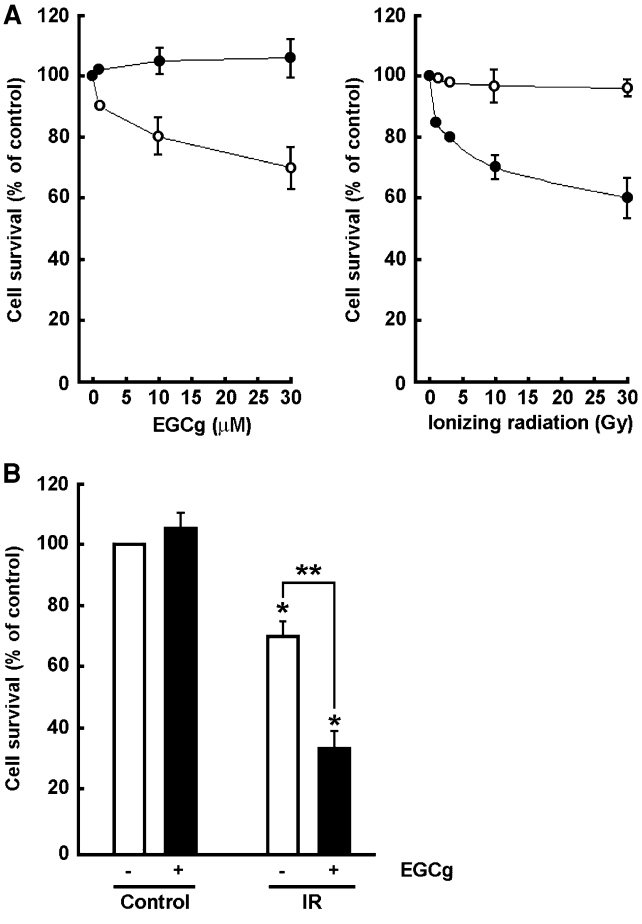

Fig. 1 Effects of EGCg treatment or ionizing radiation exposure on HBMECs' survival. (A) Subconfluent HBMEC were either treated with EGCg for 6 h in serum-free medium or exposed to a single dose of ionizing radiation (IR). Cell survival was assessed immediately after (white circles) and 48 h after (black circles) individual treatments using an automatic nuclear cell counter and Trypan blue staining. Cell survival is expressed as percent of the non-treated and non-irradiated (control) cell survival. (B) HBMEC survival assessed 48 h after combined EGCg (10 µM)/IR (10 Gy) treatments. Probability values of less than 0.05 were considered significant, and an asterisk (*) identifies such significance against untreated control. A double asterisk (**) identifies significant probability values of less than 0.05 in irradiated conditions

circles). In contrast, 48 h after treatment, cells had recovered from the EGCg treatment and no effect could be observed at this time on cell survival (Fig. 1A, left panel, black circles). HBMEC survival was also assessed after exposure to single IR doses, either immediately or after 48 h recovery. We found that low IR doses had no effect on cell survival assessed 1 h after IR (Fig. 1A, right panel, white circles). On the contrary, 48 h after IR exposure, cell survival was reduced by 30% at 10 Gy and by 40% at 30 Gy (Fig. 1A, right panel, black circles). Interestingly, HBMEC pretreated with 10 μM EGCg and exposed to a 10 Gy single IR dose showed a 70% reduction in cell survival 48 h after IR exposure (Fig. 1B). Therefore, combined EGCg/IR treatments synergistically reduced cell survival.

The reduction of HBMEC survival following combined EGCg/IR treatment is not due to changes in cell cycle phases

Cell cycle distribution was assessed in HBMEC which had been treated with 10 μM EGCg and/or irradiated at single low doses (≤10 Gy) and then left to recuperate in medium with serum for 48 h. We employed a 10 μM EGCg treatment concentration and used 10 Gy as the delivered IR dose since the combination of these treatment levels was associated with a synergistic decrease in cell survival 48 h after treatments (Fig. 1B). Discrete modulations of cell cycle phase distribution were observed in cells pretreated for 6 h with low concentrations of EGCg (Fig. 2, lower left panel). On the opposite, cell cycle phase analysis of irradiated HBMEC showed a significant accumulation of cells in G2 M phase (Fig. 2, upper right panel) and identical results were found when cells were treated with combined EGCg/IR (Fig. 2, lower right panel).

Expression of the cyclin kinase inhibitors p21 and p27 is separately induced by EGCg and IR treatments

We investigated the protein expression of the cyclin kinase inhibitors p21(CIP/Waf1) and p27(Kip), known to arrest cell cycle progression by inhibiting G1-S and G2-M transitions [37–39] (Fig. 3A, B). IR exposure (10 Gy) increased the expression of cyclin kinase inhibitors p21 and p27 2.0 to 2.4-fold over basal expression (Fig. 3B). In addition, 10 μM EGCg treatments also induced a 1.9 to 2.5-fold increase in the p21 and p27 proteins (Fig. 3B). However, the combination of EGCg/IR treatments did not further modulate p21 and p27 expression. GAPDH protein levels were not affected by EGCg treatment and/or IR exposure (Fig. 3A).

IR-induced DNA random fragmentation increases following combined EGCg/IR treatment

Forty-eight hours after treatment with EGCg and/or IR, we assessed cell cycle distribution in HBMEC. The characteristics of cell distribution in the sub-G1 region were studied on the DNA histogram obtained by flow cytometry (Fig. 2). Instead of observing only a distinct peak in the sub-G1 region representing apoptotic cells, we found an increase evenly distributed across the same region, suggesting the presence of randomly degraded DNA, a phenomenon representative of necrosis as established in the literature [40]. Quantification of the gated population found in the sub-G1 region revealed that IR and combined EGCg/IR treatments induced a 2.25-fold and almost 3.5-fold increase, respectively, in the sub-G1 population as characterized above (Fig. 4). These results prompted us to further investigate whether apoptosis might contribute to the decrease in cell survival.

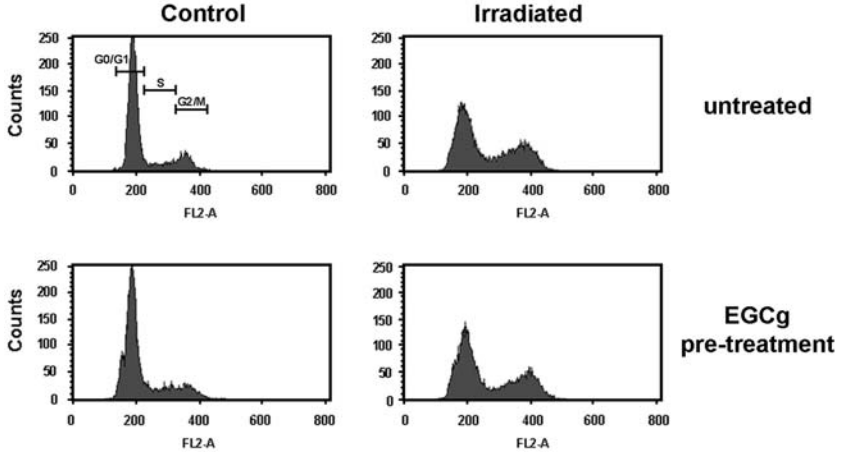

Fig. 2 Ionizing radiation's influence on HBMEC cell cycle phase distribution is not modulated by EGCg pre-treatment. Cells were harvested 48 h following 10 μM EGCg and/or 10 Gy IR treatments and cell cycle was analyzed by flow cytometry as described in the Methods section

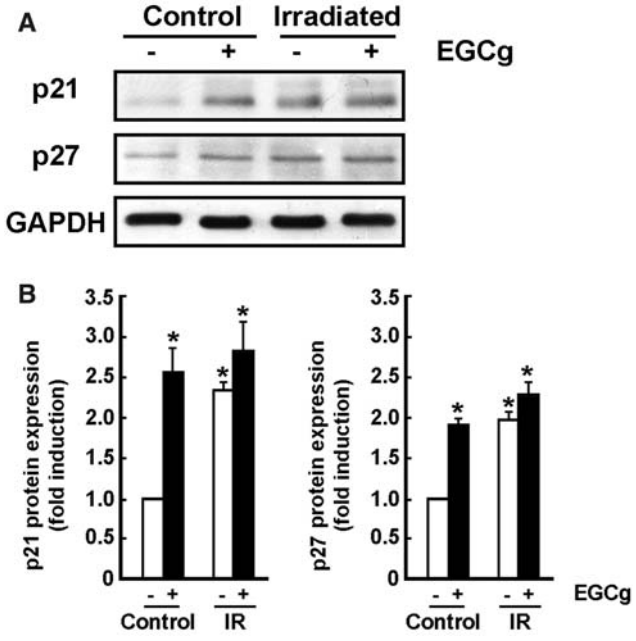

Fig. 3 Induction of cyclin kinase inhibitors p21 and p27 by EGCg treatment and IR. (A) Subconfluent HBMEC were treated with EGCg (10 μM) and/or irradiated at 10 Gy, left to recuperate at 37°C for 48 h and then harvested. Cell lysates of each condition were electrophoresed on SDS-gels and immunodetection was carried out as described in the Methods section. (B) Results from a representative experiment were normalized to GAPDH expression. Quantification of p21 and p27 protein expression was performed by scanning densitometry of samples from control cells and from HBMEC treated with EGCg and/or IR. Probability values of less than 0.05 were considered significant, and an asterisk (*) identifies such significance against untreated control

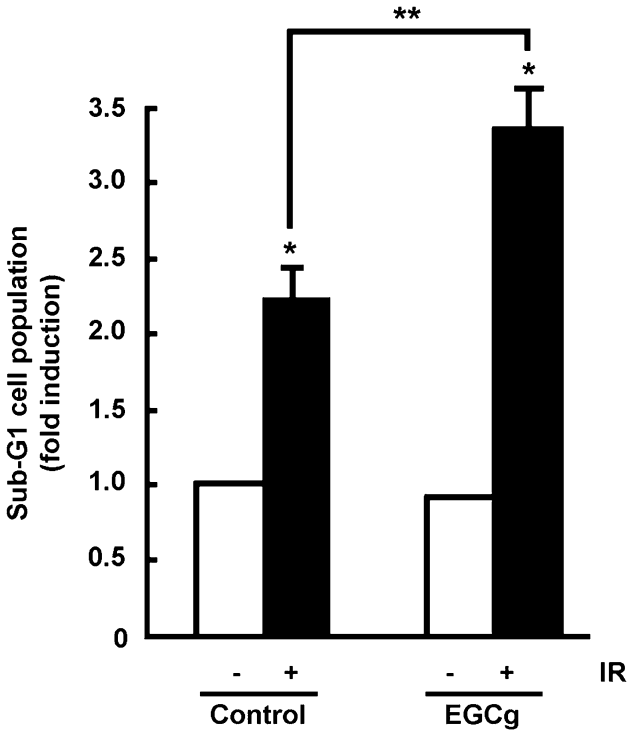

Fig. 4 Combined EGCg and ionizing radiation treatments increased sub-G1 population. Forty-eight hours after EGCg and/or IR treatments, cell cycle was assessed by flow cytometry, with specific attention to the sub-G1 region. Although IR (10 Gy) treatment induced 2.25-fold induction of the sub-G1 region content, combined EGCg (10 μM)/IR (10 Gy) treatments induced a 3.25-fold induction, suggesting that cell death is increased. Probability values of less than 0.05 were considered significant, and an asterisk (*) identifies such significance against the respective non-irradiated conditions. A double asterisk (**) identifies significant probability values of less than 0.05 in irradiated conditions

IR-induced caspase-dependent mechanisms are not increased by EGCg pre-treatment

In order to assess whether the decrease in cell survival was due to increased cell death through apoptosis, we measured the expression of pro-apoptotic proteins caspase-3, caspase-9 and cytochrome C. No significant increases in the expression of these pro-apoptotic proteins or in that of the housekeeping protein GAPDH were observed following combined EGCg/IR treatments as compared to basal expression (Fig. 5A). We also assessed apoptosis by measuring caspase-3 activity 48 h after EGCg treatment and/or IR exposure. Although exposure to EGCg slightly induced caspase-3 activity at 10 μM, IR induced a significant dose-dependent increase in caspase-3 activity (Fig. 5B, left panel). EGCg pre-treatment did not modulate the IR-induced caspase-3 activity (Fig. 5B, right panel). We next examined whether the decrease in cell survival was rather due to increased cell death through necrosis.

Combined EGCg/IR treatments increase HBMEC necrosis

HBMEC treated with EGCg and/or IR and left to recuperate for 48 h were harvested and stained with annexin-V and propidium iodide as described in the Methods section. Quantification of the population distribution throughout the four areas revealed that no significant increase occurred in early (Fig. 6A, lower right quadrant) or late apoptosis (Fig. 6A, upper right quadrant) in EGCg-treated, irradiated cells as compared to control cells. However, cell necrosis (Fig. 6A, upper left quadrant) increased 5-fold following combined EGCg/IR treatments (Fig. 6B). These results suggest that non-apoptotic pathways such as necrosis might contribute to the decrease in cell survival following combined EGCg/IR treatments and could explain the decrease in HBMEC survival.

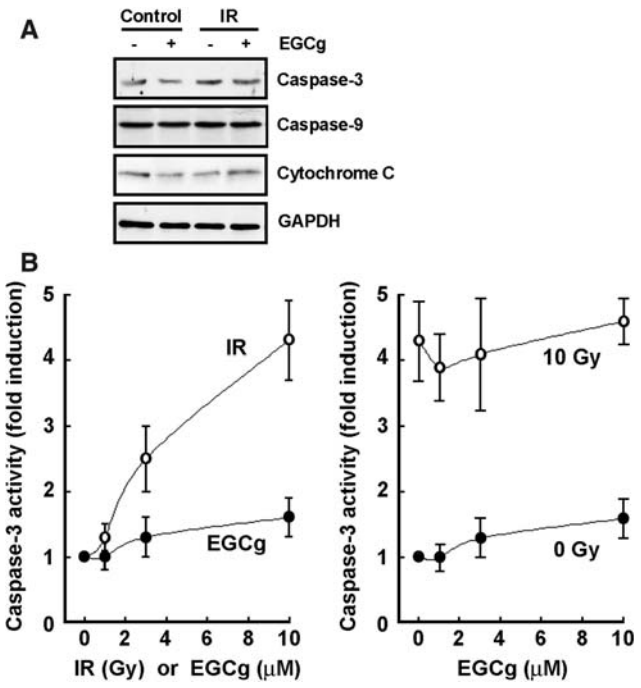

Fig. 5 IR-induced caspase-dependant mechanisms are not increased by EGCg pre-treatment. (A) HBMEC were treated with 10 μM EGCg and/or exposed to a single 10 Gy IR dose. Cells were left to recuperate for 48 h and were harvested. Cell lysates were electrophoresed on SDS-gels and immunodetection was carried out for caspase-3, caspase-9, and cytochrome C as described in the Methods section. (B) In the left panel, caspase-3 activity was measured as described in the Methods section, on harvested cells after EGCg treatment (black circles) or single radiation exposure (white circles). In the right panel, caspase-3 activity is shown for cells treated with various doses of EGCg and then followed (white circles) or not (black circles), with 10 Gy IR exposure

Discussion

We have recently shown that IR decreases in vitro cell proliferation of malignant glioma cells derived from highly vascularized brain tumors [8]. Furthermore, we also demonstrated that EGCg can enhance the effects of IR on these same cells by potentiating the decrease in cell proliferation [8]. Interestingly, malignant gliomas' proliferation, invasiveness and necrosis are directly related to their microvasculature [7]. Therefore tumor-associated EC represent a potential new treatment target. IR is capable of inducing cellular injuries to EC in vitro and in vivo [10, 14–16, 34]. However, little is known about EC injury occurring after radiation exposure and even less is known regarding EGCg's capacity to enhance the effects of IR on HBMEC. In the present study, we therefore characterized the impact of IR on HBMEC and tested whether EGCg could optimize this effect.

The HBMEC model used in this study is a surrogate model that approximates tumor-derived EC. Although one must recognize that this model does not represent glioma-derived EC, it is to our knowledge the closest in vitro model that can approximate the human brain tumor-derived EC phenotype in long-term studies. Until recently, molecular impacts on brain microvasculature functions were in fact extrapolated from studies mostly performed on human umbilical vein EC (HUVEC) [34] or bovine aortic EC (BAEC) [41]. However, microvascular EC, such as brain EC, display a selective phenotype which differs from macrovascular EC [35]. Recently, isolation of human EC from glioblastoma specimens was achieved [42, 43]. Unfortunately, primary cell cultures were found not to be suitable for long-term in vitro studies since they de-differentiated in culture and had inherently limited proliferative potential before senescence [44]. The HBMEC model thus represents a stable in vitro model since they maintain both morphological and functional characteristics of brain EC, as well as an increased proliferation rate due to their transformation with the simian virus 40 large T antigen [36]. Noteworthy, HUVEC immortalized with SV40 antigens and the catalytic subunit of human telomerase overexpress the tumor endothelial marker-1/endosialin which is regarded as the most differentially expressed molecule in tumor-derived endothelium versus normal-derived endothelium [45]. Therefore the fact that HBMEC were immortalized by transfection with SV40 allows us to further approximate the molecular impact of our study to those cells that would have acquired some transformed phenotype in the GBM tumor microenvironment.

To investigate the mechanism responsible for the synergistic EGCg/IR decrease in cell survival we first assessed changes in the cell cycle. It has been firmly established that IR results in prolongation of the cell cycle, including delays or arrests in the G1, S and G2 phases [46–49], and induction of cyclin inhibitor p21(cip/waf) [37]. Interestingly, p21(CIP/WAF) and p27(kip) have also been recognized as effectors of cell cycle arrest at the G1-S and G2-M phases of the cell cycle [37–39]. Similarly, EGCg has been shown capable of inducing G1-phase arrest of cell cycle in many cell lines [25–27], depending on the concentration and the duration of treatment. Several studies have indeed recognized that EGCg treatment induces p21 [25–27] and p27 expression [26, 50]. Interestingly, p21 may exhibit an antiapoptotic or proapoptotic effect depending on the conditions inducing its expression [51]. In our study, pre-treatment with low concentrations of EGCg (≤10 μM) during a short period of time (≤6 h) did not affect the IR-induced

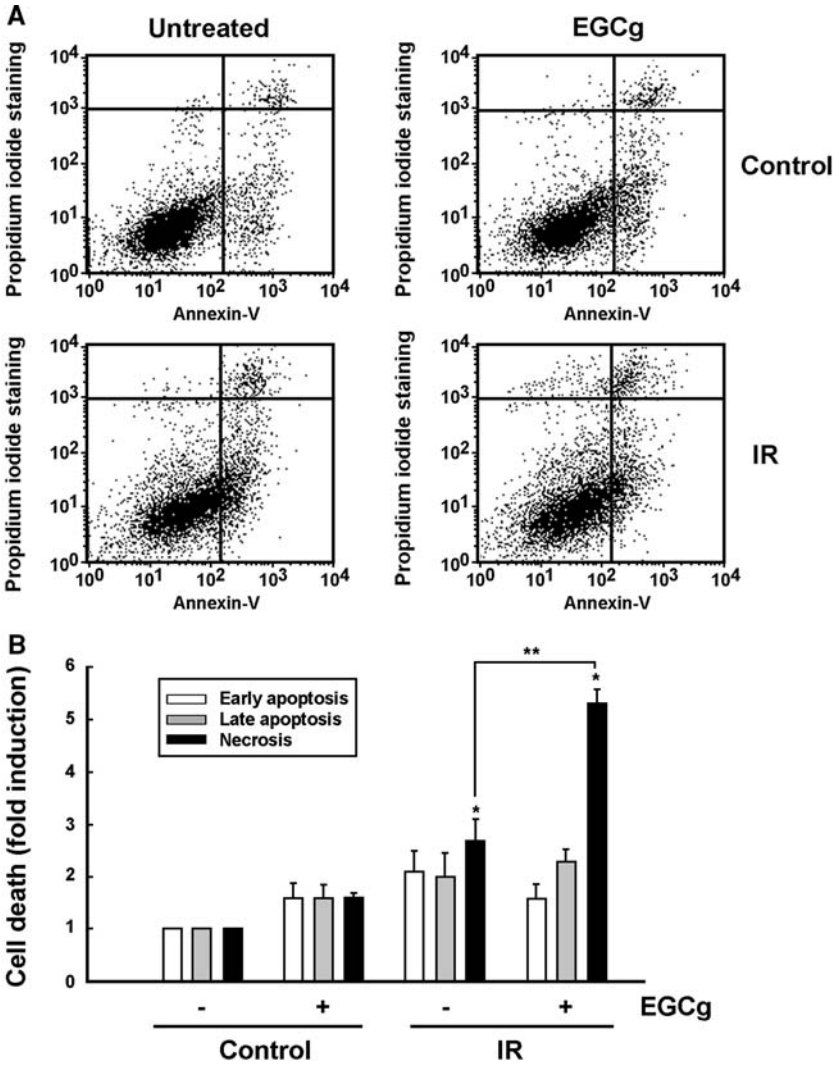

Fig. 6 Cell necrosis significantly increases following EGCg/IR combined treatments. Cell apoptosis and necrosis were analyzed, 48 h after 10 μM EGCg and/or 10 Gy IR treatments, by flow cytometry after double staining with Annexin V and propidium iodide as described in the Methods section. (A) Lower left quadrant represents viable cells; lower right quadrant, early apoptosis; upper right quadrant, late apoptosis; upper left quadrant, necrosis. (B) Bar graph illustrates the quantification performed on each quadrant from (A). Probability values of less than 0.05 were considered significant, and an asterisk (*) identifies such significance against untreated control. A double asterisk (**) identifies significant probability values of less than 0.05 in irradiated conditions

G2–M and G1–S transition arrests nor the overexpression of cyclin kinase inhibitor proteins. Therefore the cell cycle changes cannot account for the synergistic survival decrease of cells pretreated with EGCg and subsequently irradiated.

Recently, a study of total body irradiation in mice showed that the proportion of EC undergoing apoptosis in a population of cells was 20% after 12 h [16]. In light of these findings, we sought to determine whether apoptosis-mediated cell death, a late event which eliminates cells with irreparable DNA damage, could account for the synergistic EGCg/IR effect. We showed that low dose IR induced only moderate caspase-3 activity, and that HBMEC exposure to EGCg did not induce significant caspase-3 activity nor did it modulate IR-induced, caspase-dependent mechanisms. Although the late stage of apoptosis is associated with secondary necrotic cell death, primary necrotic cell death may occur in the absence of apoptotic parameters [52]. The possible contribution of non-apoptotic pathways, such as necrosis, was next investigated. We found that random DNA fragmentation, assessed by sub-G1 cell distribution, increased significantly following IR exposure and, more importantly, this effect was enhanced by combined EGCg/IR treatments. Although no significant increase in cell necrosis was observed in HBMEC treated with either EGCg or IR, the combined treatments did increase cell necrosis. These results suggest that the cell death pathways leading to necrosis may explain the synergistic effect of EGCg/IR treatments.

It is well recognized that IR is capable of inducing both apoptosis and necrosis in various tumor cell lines [52, 53]. Many factors may influence the importance of necrosis following IR. Studies have shown that necrosis is induced in tumor cells following exposure to high irradiation doses [53–55]. However, it has also been shown that human promyeloctytic leukemia cells,

irradiated with 50 Gy, died early, primarily by apoptosis while cells irradiated with 10 Gy died later, predominantly by necrosis [56]. The effect of time after radiation is controversial and probably depends on many additional factors. Some authors report that rapid cell death occurs primarily through a non-apoptotic pathway [57, 58] while others observe a dose-related increase in necrosis with some delay after exposure [23]. Furthermore, human lymphocytes exposed to X-rays for up to 20 Gy displayed no necrosis at 4 h post-IR. Although cell death was explained through apoptosis in short-term culture (4 h), the proportion of apoptotic cells did not match the increase in cell death with increasing radiation. The authors explained this discrepancy as being due to prolongation of the apoptotic process [59]. In long-term cultures, a combination of apoptosis and necrosis was apparent and explained the decrease in viability [59]. The kinetics of appearance of both apoptotic and necrotic cells in irradiated tumors is most probably influenced by cell cycle progression and by cell loss. In addition, treatment of cancer cells with chemotherapeutic agents and IR resulted in an increase in the necrotic component of cell death [60]. For example, combined treatment of a melanoma human cell line with radiation and with camptothecin, a topoisomerase I inhibitor with significant anticancer activities, induced significantly more necrotic than apoptotic cell death [60]. Interestingly, simultaneous exposure of a human leukemic cell line, EOL-1, to high concentrations of EGCg (50 μM) and IR (0–8 Gy) resulted in a synergistic decrease in cell proliferation and a synergistic increase in apoptosis and necrosis [23].

Interestingly, EGCg bears recognized antiangiogenic properties. Many mechanisms have been proposed for this, including decreased production of VEGF by tumor cells, interfering with VEGF receptor activity [33] and expression [32], and altering endothelial morphogenesis and cellular functions [33]. Therefore, VEGF survival signalling might be inhibited by EGCg, which could partially explain the enhanced results of combining radiotherapy and antiangiogenesis agents [61]. Furthermore, EGCg has been shown to sensitize various tumor cell lines to radiation and to augment the effectiveness of radiotherapy [8, 23, 24]. EGCg has also been shown to induce apoptosis in a variety of cell lines including EC lines, but at doses ranging from 20 to 100 μM over various time periods [29, 34, 62]. In our study, because EGCg pre-treatment did not, by itself, induce apoptosis or potentiate IR-induced apoptosis, increased apoptosis cannot explain the synergistic EGCg/IR decrease in cell survival.

In summary, brain tumor-associated EC represent a powerful cancer treatment target especially in highly vascularized tumors such as GBM [4]. Although the HBMEC model used in the present study does not represent glioma-derived EC, it is to our knowledge the closest in vitro model that can approximate the human brain tumor-derived EC phenotype in long-term studies. The combination of EGCg and IR treatments resulted in a synergistic delayed anti-survival effect that could be accounted for by an increase in necrosis. It can be envisioned that strategies sensitizing brain tumor vasculature to low dose IR may thus enhance the efficacy of radiotherapy. Therefore, EGCg represents a potential agent for sensitizing brain EC to radiotherapy, possibly by potentiating IR's necrotic effect.

Acknowledgments B.A. holds a Canada Research Chair in Molecular Oncology from the Canadian Institutes of Health Research. R.B. holds an Institutional UQAM Research Chair in Cancer Prevention and Treatment and the Claude Bertrand Chair of Neurosurgery (CHUM). This research was supported by the NSERC.

References

1. Laperriere N, Zuraw L, Cairncross G (2002) Cancer Care Ontario Practice Guidelines Initiative Neuro-Oncology Disease Site Group: radiotherapy for newly diagnosed malignant glioma in adults: a systematic review. Radiother Oncol 64:259–273
2. Davis FG, McCarthy BJ, Freels S, Kupelian V, Bondy ML (1999) The conditional probability of survival of patients with primary malignant brain tumors: surveillance, epidemiology, and end results (SEER) data. Cancer 85:485–491
3. Glioma Meta-analysis Trialists (GMT) Group (2002) Chemotherapy in adult high-grade glioma: a systematic review and meta-analysis of individual patient data from 12 randomised trials. Lancet 359:1011–1018
4. Brem S, Cotran R, Folkman J (1972) Tumor angiogenesis: a quantitative method for histologic grading. J Natl Cancer Inst 48:347–356
5. Folkman J (1971) Tumor angiogenesis: therapeutic implications. N Eng J Med 285:1182–1186
6. Chaudhry IH, O'Donovan DG, Brenchley PE, Reid H, Roberts IS (2001) Vascular endothelial growth factor expression correlates with tumour grade and vascularity in gliomas. Histopathology 39:409–415
7. Brem S (2003) Angiogenesis and brain tumors. In: Youmans Neurological Surgery, 5th edn. Saunders, Philadelphia (PA), pp 771–789
8. McLaughlin N, Annabi B, Bouzeghrane M, Temme A, Bahary JP, Moumdjian R, Beliveau R (2006) The survivin-mediated radioresistant phenotype of glioblastomas is regulated by RhoA and inhibited by the green tea polyphenol (−) epigallocatechin-3-gallate. Brain Research 1071:1–9
9. Hendry JH, West CM (1997) Apoptosis and mitotic cell death: their relative contributions to normal tissue and tumor radiation response. Int J Radiat Biol 71:709–719

10. Garcia-Barros M, Paris F, Cordon-Cardo C, Lyder D, Rafii S, Haimovitz-friedman A, Fuks Z, Kolesnick R (2003) Tumor response to radiotherapy regulated by endothelial cell apoptosis. Science 300:1155–1159
11. Denekamp J (1982) Endothelial cell proliferation as a novel approach to targeting tumour therapy. Br J Cancer 45:136–139
12. Bolus NE (2001) Basic review of radiation biology and terminology. J Nucl Med Technol 29:67–73
13. Coleman CN (1988) Hypoxia in tumors: a paradigm for the approach to biochemical and physiologic heterogeneity. J Nat Cancer Inst 80:310–317
14. Maj JG, Paris F, Haimovitz-Friedman A, Venkatraman E, Kolesnick R, Fuks Z (2003) Microvascular function regulates intestinal crypt response to radiation. Cancer Res 63:4338–4441
15. Paris F, Fuks Z, Kang A, Capodieci P, Juan G, Ehleiter D, Haimovitz-Friedman A, Cordon-Cardo C, Kolesnick R (2001) Endothelial apoptosis as the primary lesion initiating intestinal radiation damage in mice. Science 293:293–297
16. Pena LA, Fuks Z, Kolesnick RN (2000) Radiation-induced apoptosis of endothelial cells in the murine central nervous system: protection by fibroblast growth factor and sphingomyelinase deficiency. Cancer Res 60:321–327
17. Fuks Z. Persaud RS, Alfieri A, McLoughlin M, Ehleiter D, Schwartz JP,Seddon AP, Cordon-Cardo C, Haimovitz-Friedman A (1994) Basic fibroblast growth factor protects endothelial cells against radiation-induced programmed cell death in vitro and in vivo. Cancer Res 54:2582–2590
18. Browder T, Butterfield CE, Kraling BM, Shi B, Marshall B, O'Reilly MS, Folkman J (2000) Antiangiogenic scheduling of chemotherapy improves efficacy against experimental drug-resistant cancer. Cancer Res 60:1878–1886
19. Edinger AL, Thompson CB (2004) Death by design: apoptosis, necrosis and autophagy. Curr Opin Cell Biol 16:663–669
20. Stupp R, Mason WP, van der Bent MJ, Weller M, Fisher B, Taphoorn MJ, Belanger K, Brandes AA, Marosi C, Bogdahn U, Curschmann J, Janzer RC, Ludwin SK, Gorlia T, Allgeier A, Lacombe D, Cairncross JG, Eisenhauer E, Mirimanoff RO, European Organisation for Research and Treatment of Cancer Brain Tumor and Radiotherapy Groups; National Cancer Institute of Canada Clinical Trials (2005) Group Radiotherapy plus concomitant and adjuvant temozolomide for glioblastoma. N Engl J Med 352:987–996
21. Schuuring J, Bussink J, Bernsen HJ, Peeters W, van Der Kogel AJ (2005) Irradiation combined with SU5416: microvascular changes and growth delay in a human xenograft glioblastoma tumor line. Int J Radiat Oncol Biol Phys 61:529–534
22. Chendil D, Ranga RS, Meigooni D, Sathishkumar S, Ahmed MM (2004) Curcumin confers radiosensitizing effect in prostate cancer cell line PC-3. Oncogene 23:1599–1607
23. Baatout S, Derradji H, Jacquet P, Mergeay M (2005) Increased radiation sensitivity of an eosinophilic cell line following treatment with epigallocatechin-gallate, resveratrol and curcuma. Int J Mol Med 15:337–352
24. Baatout S, Jacquet P, Derradji H, Ooms D, Michaux A, Mergeay M (2004) Study of the combined effect of X-irradiation and epigallocatechin-gallate (a tea component) on the growth inhibition and induction of apoptosis in human cancer cell lines. Oncol Rep 12:159–167
25. Kim CH, Moon SK (2005) Epigallocatechin-3-gallate causes the p21/WAF1-mediated G(1)-phase arrest of cell cycle and inhibits matrix metalloproteinase-9 expression in TNF-alpha-induced vascular smooth muscle cells. Arch Biochem Biophys 435:264–272
26. Gupta S, Hussain T, Mukhtar H (2003) Molecular pathway for (−)-epigallocatechin-3-gallate-induced cell cycle arrest and apoptosis of human prostate carcinoma cells. Arch Biochem Biophys 410:177–185
27. Ahmad N, Cheng P, Mukhtar H (2000) Cell cycle dysregulation by green tea polyphenol epigallocatechin-3-gallate. Biochem Biophys Res Commun 275:328–334
28. Yokoyama S, Hirano H, Wakimaru N, Sarker KP, Kuratsu J (2001) Inhibitory effect of epigallocatechin-gallate on brain tumor cell lines in vitro. Neuro-oncol 3:22–28
29. Fassina G, Vene R, Morini M, Minghelli S, Benelli R, Noonan DM, Albini A (2004) Mechanisms of inhibition of tumor angiogenesis and vascular tumor growth by epigallocatechin-3-gallate. Clin Cancer Res 10:4865–4873
30. Annabi B, Bouzeghrane M, Moumdjian R, Moghrabi A, Beliveau R (2005) Probing the infiltrating character of brain tumors: inhibition of RhoA/ROK-mediated CD44 cell surface shedding from glioma cells by the green tea catechin EGCg. J Neurochem 94:906–916
31. Pilorget A, Berthet V, Luis J, Moghrabi A, Annabi B, Beliveau R (2003) Medulloblastoma cell invasion is inhibited by green tea (−)epigallocatechin-3-gallate. J Cell Biochem 90:745–755
32. Kojima-Yuasa A, Hua JJ, Kennedy DO, Matsui-Yuasa I (2003) Green tea extract inhibits angiogenesis of human umbilical vein endothelial cells through reduction of expression of VEGF receptors. Life Sci 73:1299–1313
33. Lamy S, Gingras D, Béliveau R (2002) Green tea catechins inhibit vascular endothelial growth factor receptor phosphorylation. Cancer Res 62:381–385
34. Annabi B, Lee YT, Martel C, Pilorget A, Bahary JP, Beliveau R (2003) Radiation induced-tubulogenesis in endothelial cells is antagonized by the antiangiogenic properties of green tea polyphenol (−)epigallocatechin-3-gallate. Cancer Biol Ther 2:642–649
35. Stins MF, Gilles F, Kim KS (1997) Selective expression of adhesion molecules on human brain microvascular endothelial cells. J Neuroimmunol 76:81–90
36. Greiffenberg L, Goebel W, Kim KS, Weiglein I, Bubert A, Engelbrecht F, Stins M, Kuhn M (1998) Interaction of *Listeria monocytogenes* with human brain microvascular endothelial cells: InlB-dependent invasion, long-term intracellular growth, and spread from macrophages to endothelial cells. Infect Immun 66:5260–5267
37. Kim HS, Cho HJ, Cho HJ, Park SJ, Park KW, Chae IH, Oh BH, Park YB, Lee MM (2004) The essential role of p21 in radiation-induced cell cycle arrest of vascular smooth muscle cell. J Mol Cell Cardiol 37:871–880
38. Maeda T, Chong MT, Espino RA, Chua PP, Cao JQ, Chomey EG, Luong L, Tron VA (2002) Role of p21(Waf-1) in regulating the G1 and G2/M checkpoints in ultraviolet-irradiated keratinocytes. J Invest Dermatol 119:513–521
39. Toyoshima H, Hunter T (1994) p27, a novel inhibitor of G1 cyclin-Cdk protein kinase activity, is related to p21. Cell 78:67–74
40. Ormerod MG (2002) Investigating the relationship between the cell cycle and apoptosis using flow cytometry. J Immunol Meth 265:73–80
41. Tanaka T (1997) Effect of adenoviral-mediated thymidine kinase transduction and ganciclovir therapy on tumor-associated endothelial cells. Neurol Med Chir (Tokyo) 37:730–737
42. Bian XW, Jiang XF, Chen JH, Bai JS, Dai C, Wang QL, Lu JY, Zhao W, Xin R, Liu MY, Shi JQ, Wang JM (2006) Increased angiogenic capabilities of endothelial cells from microvessels of malignant human gliomas. Int Immunopharmacol 6:90–99

43. Charalambous C, Hofman FM, Chen TC (2005) Functional and phenotypic differences between glioblastoma multiforme-derived and normal human brain endothelial cells. J Neurosurg 102:699–705
44. Bian C, Zhao K, Tong GX, Zhu YL, Chen P (2005) Immortalization of human umbilical vein endothelial cells with telomerase reverse transcriptase and simian virus 40 large T antigen. J Zhejiang Univ Sci B 6:631–636
45. Tentori L, Vergati M, Muzi A, Levati L, ruffini F, Forini O, Vernole P, Lacal PM, Graziani G (2005) Generation of an immortalized human endothelial cell line as a model of neovascular proliferating endothelial cells to assess chemosensitivity to anticancer drugs. Int J Oncol 27:525–535
46. Zhao H, Spitz MR, Tomlinson GE, Zhang H, Minna JD, Wu X (2001) Gamma-radiation-induced G2 delay, apoptosis, and p53 response as potential susceptibility markers for lung cancer. Cancer Res 61:7819–7824
47. Hwang A, Muschel RJ (1998) Radiation and the G2 phase of the cell cycle. Radiat Res 150(Suppl):52–59
48. Schwartz D, Almog N, Peled A, Goldfinger N, Rotter V (1997) Role of wild-type p53 in the G2 phase: regulation of the gamma-irradiation-induced delay and DNA repair. Oncogene 15:2597–2607
49. Bernhard EJ, Maity A, Muschel RJ, McKenna WG (1995) Effects of ionizing radiation on cell cycle progression. A review. Radiat Environ Biophys 34:79–83
50. Liang YC, Lin-Shiau SY, Chen CF, Lin JK (1999) Inhibition of cyclin-dependent kinases 2 and 4 activities as well as induction of Cdk inhibitors p21 and p27 during growth arrest of human breast carcinoma cells by (−)-epigallocatechin-3-gallate. J Cell Biochem 75:1–12
51. Nakamura K, Arai D, Fukuchi K (2004) Identification of the region required for the antiapoptotic function of the cyclin kinase inhibitor, p21. Arch Biochem Biophys 431:47–54
52. Vanden Berghe T, Denecker G, Brouckaert G, Vadimovisch Krysko D, D'Herde K, Vandenabeele P (2004) More than one way to die: methods to determine TNF-induced apoptosis and necrosis. Meth Mol Med 98:101–126
53. Shimamura H, Sunamura M, Tsuchihara K, Egawa S, Takeda K, Matsuno S (2005) Irradiated pancreatic cancer cells undergo both apoptosis and necrosis, and could be phagocytized by dendritic cells. Eur Surg Res 37:228–234
54. Rainaldi G, Ferrante A, Indovina PL, Santini MT (2003) Induction of apoptosis or necrosis by ionizing radiation is dose-dependent in MG-63 osteosarcoma multicellular spheroids. Anticancer Res 23:2505–2518
55. Nagata S, Obana A, Gohto Y, Nakajima S (2003) Necrotic and apoptotic cell death of human malignant melanoma cells following photodynamic therapy using an amphiphilic photosensitizer, ATX-S10(Na). Lasers Surg Med 33:64–70
56. Dynlacht JR, Earles M, Henthorn J, Roberts ZV, Howard EW, Seno JD, Sparling D, Story MD (1999) Degradation of the nuclear matrix is a common element during radiation-induced apoptosis and necrosis. Radiat Res 152:590–603
57. Kurita H, Ostertag CB, Baumer B, Kopitzki K, Warnke PC (2000) Early effects of PRS-irradiation for 9L gliosarcoma: characterization of interphase cell death. Minim Invasive Neurosurg 43:197–200
58. Olive PL, Vikse CM, Vanderbyl S (1999) Increase in the fraction of necrotic, not apoptotic, cells in SiHa xenograft tumours shortly after irradiation. Radiother Oncol 50:113–119
59. Payne CM, Bjore CG Jr, Schultz DA (1992) Change in the frequency of apoptosis after low- and high-dose X-irradiation of human lymphocytes. J Leukoc Biol 52:433–440
60. Quto b SS, Ng CE (2002) Comparison of apoptotic, necrotic and clonogenic cell death and inhibition of cell growth following camptothecin and X-radiation treatment in a human melanoma and a human fibroblast cell line. Cancer Chemother Pharmacol 49:167–175
61. Siemann DW, Horsman MR (2004) Targeting the tumor vasculature: a strategy to improve radiation therapy. Expert Rev Anticancer Ther 4:321–327
62. Yoo HG, Shin BA, Park JC, Kim HS, Kim WJ, Chay KO, Ahn BW, Park RK, Ellis LM, Jung YD (2002) Induction of apoptosis by the green tea flavonol (−)-epigallocatechin-3-gallate in human endothelial ECV 304 cells. Anticancer Res 22:3373–3378